

# High-Force Generation Is a Conserved Property of Type IV Pilus Systems<sup>∇</sup>

Martin Clausen,<sup>1</sup> Vladimir Jakovljevic,<sup>2</sup> Lotte Søggaard-Andersen,<sup>2</sup> and Berenike Maier<sup>1\*</sup>

Department for Biology, Westfälische Wilhelms Universität, Schlossplatz 5, 48149 Münster, Germany,<sup>1</sup> and Department of Ecophysiology, Max Planck Institute for Terrestrial Microbiology, Karl-von-Frisch-Straße, 35043 Marburg, Germany<sup>2</sup>

Received 24 March 2009/Accepted 5 May 2009

**The type IV pilus (T4P) system of *Neisseria gonorrhoeae* is the strongest linear molecular motor reported to date, but it is unclear whether high-force generation is conserved between bacterial species. Using laser tweezers, we found that the average stalling force of single-pilus retraction in *Myxococcus xanthus* of  $149 \pm 14$  pN exceeds the force generated by *N. gonorrhoeae*. Retraction velocities including a bimodal distribution were similar between *M. xanthus* and *N. gonorrhoeae*, but force-dependent directional switching was not. Force generation by pilus retraction is energized by the ATPase PilT. Surprisingly, an *M. xanthus* mutant lacking PilT apparently still retracted T4P, although at a reduced frequency. The retraction velocity was comparable to the high-velocity mode in the wild type at low forces but decreased drastically when the force increased, with an average stalling force of  $70 \pm 10$  pN. Thus, *M. xanthus* harbors at least two different retraction motors. Our results demonstrate that the major physical properties are conserved between bacteria that are phylogenetically distant and pursue very different lifestyles.**

Type IV pili (T4P) are among the most widespread cell surface appendages in bacteria and have been found in beta-, gamma-, delta-, and epsilonproteobacteria and cyanobacteria, as well as in firmicutes (27). As opposed to other filamentous surface structures, T4P are highly dynamic structures and undergo cycles of extension and retraction (22, 30, 34). During the retraction step, sufficient force is generated to pull a bacterial cell forward in a type of surface movement referred to as twitching motility (30). The dynamic behavior is central to most of the functions of T4P, which in addition to cell motility, include surface adhesion, horizontal gene transfer, biofilm formation, and protein secretion (3).

T4P are thin (5- to 8-nm) flexible filaments with a length of several micrometers (7). A core set of 10 proteins is conserved between different T4P systems and is required for T4P dynamics in *Myxococcus xanthus*, *Pseudomonas aeruginosa*, *Neisseria gonorrhoeae*, *Neisseria meningitidis*, and *Synechocystis* sp. strain PCC6803 (24, 27). Genetic and biochemical data suggest that the proteins required for T4P function interact to form a complex that spans the cell envelope (2, 9, 10, 14, 28). The molecular mechanism underlying the assembly of T4P involves the incorporation of pilin subunits in the base of the pilus (8) from a reservoir in the cytoplasmic membrane (15, 30), and retraction involves the removal and transfer of pilin subunits from the pilus base into the cytoplasmic membrane (23). Genetic and biochemical evidence suggest that assembly of T4P is energized by ATP hydrolysis by the assembly ATPase PilB (PilF in *Neisseria* spp.) (15, 29) and that T4P retraction is energized by ATP hydrolysis by the retraction ATPase PilT (5, 11, 15).

The soil-dwelling bacterium *M. xanthus* (a rod-shaped bacterium belonging to the deltaproteobacteria) requires T4P-dependent motility for the formation of spreading colonies in

vegetative cells and fruiting bodies in starving cells. T4P extension and retraction have not been quantified in *M. xanthus*; however, indirect evidence for T4P retraction was obtained by characterizing the “jiggling” movement of isolated, individual *M. xanthus* cells adhering to polystyrene-coated surfaces (34).

The dynamics and force generation of individual T4P have been characterized in detail in the human pathogen *N. gonorrhoeae* (6, 19–21), a diplococcus belonging to the betaproteobacteria. Generation of high forces in the range of 110 pN is a remarkable quality of T4P retractions in *N. gonorrhoeae* (21). It has been suggested that high-force generation may have evolved with the “lifestyle” of *N. gonorrhoeae* to induce signaling processes in the host cells during infections and to induce cytoprotection and cytoskeletal rearrangements (13). Here, we show that T4P retractions in *M. xanthus*, which lives in an entirely different habitat, has a different morphology, and is phylogenetically distant from *N. gonorrhoeae*, generate high forces in the range of 150 pN. On the basis of these observations, we suggest that high-force generation and bimodal velocity distributions are inherent properties of all T4P systems independent of phylogeny and bacterial lifestyle. Intriguingly, retractions still occurred at a low frequency in an *M. xanthus* strain lacking PilT, providing evidence for a PilT-independent retraction mechanism in *M. xanthus*. The physical characteristics of the PilT-independent T4P retractions were distinct from those in a PilT<sup>+</sup> strain.

## MATERIALS AND METHODS

**Bacterial strains and growth media.** The following strains of *M. xanthus* were used: wild-type (wt) DK1622 (16), the isogenic  $\Delta pilA$  strain DK10410 (39), the isogenic  $\Delta pilT$  strain DK10409 (15, 39), and the isogenic *romR::nptIII* strain SA1128 (18). The  $\Delta pilT$  allele encodes a truncated protein of 82 amino acids compared to the 372 amino acids of PilT (39). Cells were grown in liquid medium or on 1.5% agar containing 1% CTT as described previously (31). For retraction experiments bacteria were grown to an optical density at 600 nm of 0.3 at 32°C and 230 rpm and then transferred to a polystyrene-coated cover slide.

**Experimental setup.** Retraction experiments were performed in 1% CTT at 32°C. The bacteria were immobilized by attachment to a polystyrene-coated cover slide. For retraction experiments, a suspension of cells and 2- $\mu$ m carboxylated polystyrene beads (Polysciences) was mounted on a microscope slide and

\* Corresponding author. Mailing address: Department for Biology, Westfälische Wilhelms Universität, Schlossplatz 5, 48149 Münster, Germany. Phone: 49 251 8323920. Fax: 49 251 8324723. E-mail: maierb@uni-muenster.de.

<sup>∇</sup> Published ahead of print on 8 May 2009.

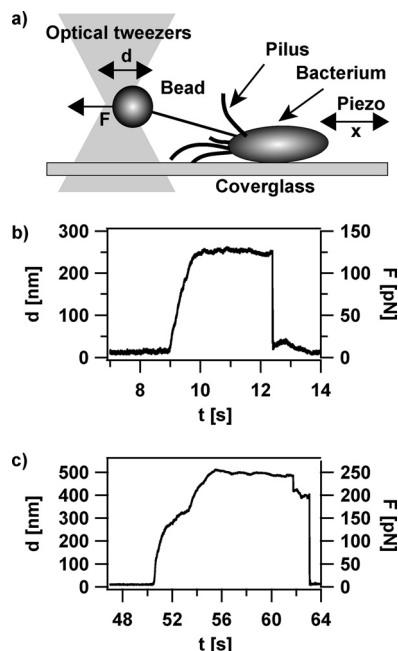


FIG. 1. Experimental setup and force generation during T4P retraction. (a) Sketch of the experimental setup. A cell was immobilized on a polystyrene-coated cover slide. When a T4P bound to the bead in the laser trap and retracted, it displaced the bead by a distance  $d$  from the center of the trap. At a preset threshold,  $d_{set}$ , the force feedback (Fig. 3a) could be triggered by moving the piezo table by a distance  $x$  to maintain  $d$  at a constant value. (b and c) Typical deflection,  $d$ , of the bead during pilus retraction as a function of time in the wt (DK1622).  $F$ , force;  $t$ , time.

sealed. Only cells that adhered to the polystyrene surface were selected. Using laser tweezers (6), we positioned a bead next to a bacterium (Fig. 1a). Eventually, the bacterium retracted a pilus that was bound to the bead in the trap. Due to the retraction, the bead was pulled out of the center of the laser trap. We measured this displacement,  $d$ , of the bead using a four-quadrant photodiode. For small values of  $d$ , i.e., small deflections, the force acting on the bead is proportional to the deflection and allows the determination of the force acting on the T4P after calibration of the trap stiffness. Likewise, measuring the deflection as a function of time allows the determination of the T4P retraction rate/velocity. The noise of raw data was reduced by applying a notch filter at 42 Hz and a moving average (1-ms box). The mean value and errors of stalling forces were determined by a robust bootstrap analysis using the Tukey method in IGOR Pro 6.04 (WaveMetrics).

For the analysis of the T4P dynamics, the data were down-sampled and differentiated. The curves were investigated at a temporal resolution of 10 ms for pausing and elongation with a velocity threshold of 150 nm/s using the direction prior to the force feedback activation. Since we then found that the main mode of pilus dynamics was retraction, requiring a lower temporal resolution, we reanalyzed the data again at a temporal resolution of 50 ms for the generation of the velocity histograms. This increased averaging of the data and led to higher resolution of the histograms. Clausen et al. have presented a more detailed discussion of the data analysis (6). For each force, the data points from all events of one strain were summarized in a histogram with 100-nm/s bin width. Peak positions were determined by fitting single or double Gaussians, unless velocities were close to the pausing threshold. In that case, the velocity was determined from the average over a global fit to the retraction curves.

For force feedback measurements with forces up to 60 pN, we used a stiffness of 0.2 pN/nm, and for exceeding forces, we used a stiffness of 0.5 pN/nm. Stalling forces were also determined at 0.5 pN/nm.

**Sequence alignment.** The sequences were aligned using ClustalX V. 1.81, (35) using the default parameters (Gonnet matrix, 10-point gap initiation, and 0.2-point gap extension). The resulting alignment was used to generate a bootstrapped neighbor-joining tree (1,000 iterations). The tree was visualized using Treedyn (4).

## RESULTS

**T4P retraction in *M. xanthus*.** To characterize the kinetics and force generation of T4P retraction in *M. xanthus*, we adapted an assay previously established for characterizing retraction kinetics and force generation by single T4P in *N. gonorrhoeae* (6) (Fig. 1a). Using *M. xanthus* strain DK1622, which served as a wt in these experiments, we observed that isolated cells close to a bead caused the displacement of the bead (Fig. 1b). These data revealed that *M. xanthus* actively retracts T4P and confirmed that cell-cell contact is not a prerequisite for T4P retraction in *M. xanthus*, as had been proposed in earlier studies (34). However, we cannot exclude the possibility that T4P retraction activity is different in *M. xanthus* cells in close contact.

In addition to the T4P-dependent motility system, *M. xanthus* harbors a second motility system, the A motility system (12). T4P and the A motility system operate independently of each other (12); however, they generate force in the same direction (17, 32). To verify that the bead movements observed reflected retractions of functional T4P, we determined whether the mutant strain SA1128, which is deficient in the A motility system due to a mutation in the *romR* gene, caused bead deflections. As expected, the *romR* mutant caused bead deflections similar to those of the wt (data not shown), indicating that A motility was not responsible for the observed bead displacement.

Next, we sought to determine whether a mutant (DK10410) that is unable to synthesize T4P due to a deletion of the *pilA* gene, which codes for the T4P subunit (38), caused bead deflections. As previously reported (34), DK10410 was unable to adhere to the polystyrene-coated coverslips and the polystyrene beads (data not shown), and therefore, the strain did not allow us to conclude whether the bead deflections observed in the wt were dependent on functional T4P. Instead, we analyzed the strain DK10409, which carries a deletion of the *pilT* gene coding for the ATPase responsible for retraction of T4P (39).  $\Delta pilT$  mutants still assemble T4P; however, these T4P have been reported to be paralyzed based on an agar plate motility assay (39). Unexpectedly,  $\Delta pilT$  mutants still caused bead deflections; however, the frequency of the deflections (i.e., the number of retraction events during a period of time) was reduced sevenfold compared to that of the wt, and the characteristics of the deflections were different from those caused by the wt (see below). These results clearly demonstrate that the retractions of the microbeads in the laser tweezers were caused by T4P.

**The stalling force of T4P retraction in *M. xanthus* is  $149 \pm 14$  pN.** To measure the stalling force of T4P in wt *M. xanthus*, we used the laser tweezers without force feedback. As the T4P pulled on the bead in the laser trap, the position of the bead was tracked at approximately 3-nm accuracy, and the force was derived from the deflection of the bead from the center of the laser tweezers. We observed that the velocity of T4P retraction decreased with increasing force applied by the laser tweezers (Fig. 1b and c). At a characteristic force (stalling force), the deflection of the bead from the center of the laser trap did not increase significantly. We defined the stalling force as the force at which the velocity of T4P retraction dropped by at least 1

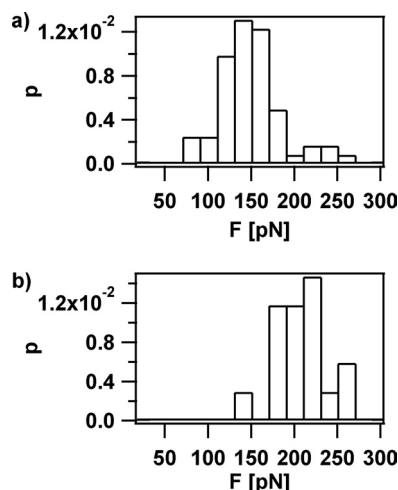


FIG. 2. Histogram of stalling forces of T4P in the wt (DK1622). Stalling events were classified into (a) 61 events containing no pause between onset of the retraction and the final plateau (Fig. 1b) and (b) 17 events containing a pause at an intermediate force level (Fig. 1c). Forces ( $F$ ) exceeding 220 pN are systematically underestimated due to limited force generation of the laser tweezers.  $p$ , normalized number of stalling events.

order of magnitude compared to the retraction velocity at 15 pN for at least 100 ms.

Interestingly, retraction events starting from zero force showed either one (Fig. 1b) ( $\sim 80\%$ ) or two (Fig. 1c) ( $\sim 20\%$ ) successive stalling events. Events starting from nonzero forces were excluded from the analysis, since in that case, the number of plateaus before the stalling could not be determined. We plotted the force histogram of single stalling events (Fig. 2a) and found that these stalling events were distributed like a Gaussian around 144 pN with a fitting error of  $\pm 1$  pN, in good agreement with the average of  $149 \pm 14$  pN, indicating that the stalling force of an individual pilus is  $149 \pm 14$  pN. The residual peak at 220 pN in Fig. 2a is most likely attributable to two pili retracting simultaneously. This interpretation was further supported by plotting a histogram of the stalling events that succeeded a stalling event at lower force (Fig. 2b). Sixty-five percent of these stalling events occurred at forces exceeding 200 pN, and 90% exceeded 180 pN. This observation strongly suggests that an individual pilus retracted until its stalling force was reached (the plateau in Fig. 1c) and that subsequently a second pilus bound and retracted until it reached the length of the first pilus. The simultaneous retraction of two pili of similar lengths generated forces exceeding 220 pN and can account for the high-force peak. The observations that the two force levels are well separated and that most of the stalling events during retractions generating two force levels were well separated in time support the notion that we observed retraction of individual T4P before the plateau was reached. We thus conclude that the average stalling force of an individual T4P is  $149 \pm 14$  pN.

**T4P retraction velocity is bimodal at low forces.** For measurements of T4P retractions at a constant force, a computer-controlled feedback was triggered at a preset threshold (Fig. 3a). Then, the bacterium was displaced by a distance  $x(t)$  to keep the force constant by keeping the distance between the

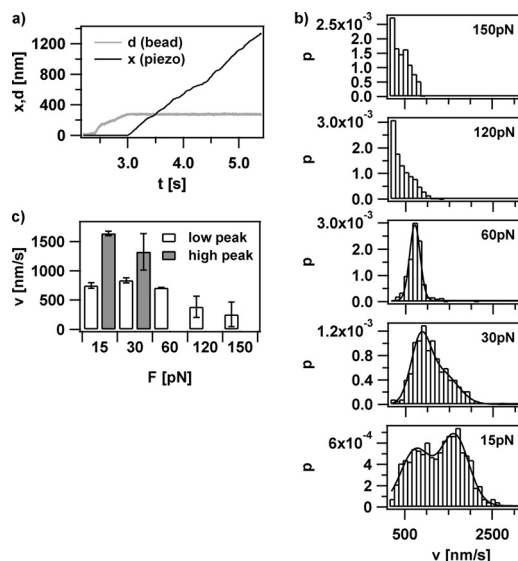


FIG. 3. Retraction velocities at constant force. (a) Typical length change  $x$  of a single T4P of the wt (DK1622) as a function of time ( $t$ ) at a fixed force of 150 pN. When a T4P bound to the bead in the laser trap and retracted, it displaced the bead by a distance  $d$  from the center of the trap. At a predefined distance  $d_{set}$  corresponding to a force  $F$ , the feedback was triggered, which moved the piezo table to keep  $d$  constant. (b) Histogram of velocities at constant force for the wt from 98 retraction curves. The average track length was about 1 second. (c) Retraction velocities obtained from panel b by fitting of a double Gaussian (15 and 30 pN) and a single Gaussian (60 pN) and by fitting of a line to all curves and averaging (120 and 150 pN). The error bars indicate standard deviations of the mean velocities.

center of the laser trap and the bead  $d$  constant. The assay allowed us to follow the dynamics of a single T4P for several seconds while applying a constant force. Due to the force clamp, no elastic effects interfered with the determination of velocities and lengths.

We analyzed the velocity of T4P length change and the probability of pausing and T4P elongation by dissecting the data with a time resolution of 10 ms for elongation and pause detection and 50 ms for velocity histograms. A histogram of the T4P retraction velocity ( $v$ ) at 15 pN showed bimodality, with two distinct peaks at a  $v$  of  $749 \pm 49$  nm/s and a  $v$  of  $1,637 \pm 38$  nm/s (Fig. 3b and c). When the force was set to 30 pN, the high-velocity peak shifted to lower values and dropped in amplitude, while the low-velocity peak remained largely unaffected. At 60 pN, only the low-velocity peak at a  $v$  of  $710 \pm 5$  nm/s remained. As the force was further increased to 150 pN, the average velocity strongly decreased to a  $v$  of  $257 \pm 209$  nm/s. At high forces in the range of 120 to 150 pN, some of the retraction motors were very close to stalling while others still had a significant velocity. This resulted in a large uncertainty, in agreement with the width of the distribution of stalling forces (Fig. 2). This is consistent with events having either one or two T4P pulling, since at these forces, the dependence of the velocity on the load is very strong. The bimodal velocity distribution at low forces cannot be explained by two T4P pulling simultaneously. If the bimodal distribution was caused by retraction of either one or two pili, then the velocity of the high-velocity mode at 30 pN would have to agree with that of

the low-velocity mode at 15 pN, since at 30 pN, each of the two pili would have to work against 15 pN. This argument is inconsistent with our data (Fig. 3c). Moreover, the velocity distribution is bimodal at low force, where velocities are high and therefore the probability for binding of multiple pili is low.

To assess whether A motility introduced an error into the velocity measurement of T4P retraction, we quantified the retraction velocity in a *romR* mutant. The velocities of retractions in the *romR* mutant were slightly higher than in the wt (data not shown). We characterized the distribution of retraction velocities in SA1128 while applying a constant force of 15 pN, 30 pN, or 60 pN to the bead. The distribution of velocities was similar to that in the wt but shifted toward higher velocities by an average value of  $\sim 100$  nm/s (data not shown). This discrepancy is most likely due to the movement of individual wt cells toward the bead by means of the A motility system, whose velocity is in the range of 60 nm/s (33). Therefore, with our setup, the velocity of wt T4P retraction is slightly underestimated due to A motility, but since the velocity difference is small, we neglected the correction throughout this work.

**The directional-switching dynamics of T4P is not conserved between *M. xanthus* and *N. gonorrhoeae*.** In *N. gonorrhoeae*, the application of high external forces to retracting T4P induces a switch to the T4P elongation mode (6, 20). Interestingly, in *M. xanthus*, a similar force-induced switch to elongation was not observed even at 150 pN, and retraction proceeded highly processively, e.g., at a force of  $\leq 60$  pN, elongation events and pauses were quantified to occur at less than 1% of the total time of pilus retraction at each force. We observed very different dynamic behaviors near the stalling force. The average retraction velocity decreased in *M. xanthus* T4P when the force was increased (Fig. 3). The average retraction velocity did not decrease in *N. gonorrhoeae* T4P when the force was increased; however, the probability of T4P elongation increased, effectively leading to stalling (6). Directional switching from retraction to elongation occurred at two distinct time scales of  $\sim 10$  ms and  $\sim 100$  to 1,000 ms. Although we cannot exclude directional switching in *M. xanthus* at a time scale shorter than our experimental resolution, we can exclude directional switching at a time scale of  $\sim 100$  to 1,000 ms. These observations suggest that force-dependent switching from retraction to elongation is not an inherent property of all T4P systems. In *N. gonorrhoeae*, T4P retraction has been suggested to induce signaling processes during infections. We speculate that the force-dependent directionality switching in *N. gonorrhoeae* has evolved as a mechanism to adjust tension during the infection process. On the other hand, T4P retraction in *M. xanthus* may serve only to drive motility, and therefore, force-dependent directionality switching may not be needed.

**Deletion of *pilT* results in increased retraction velocity but in decreased stalling force.** As mentioned above, we unexpectedly observed retractions in the  $\Delta pilT$  mutant (DK10409). We analyzed the velocity distribution of the PilT-independent retraction in the  $\Delta pilT$  mutant at constant external forces and observed at 15 pN only a single peak similar ( $v = 1,599 \pm 33$  nm/s) to the high-velocity mode in the wt (DK1622) (Fig. 4a). Thus, on average, the retraction velocity was higher in the  $\Delta pilT$  mutant than in the wt. At increasing force, the average velocity was lower in the  $\Delta pilT$  mutant than in the wt (Fig. 4b). The stalling force in the  $\Delta pilT$  mutant was  $70 \pm 10$  pN, with a

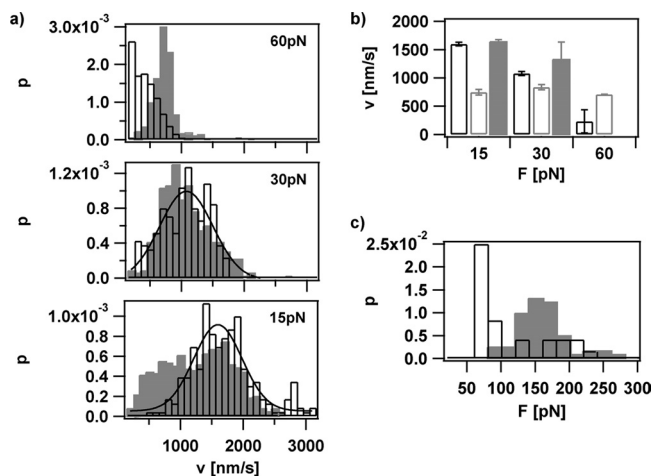


FIG. 4. T4P retraction velocity in the  $\Delta pilT$  mutant. (a) Histogram of retraction velocities at constant force. DK1622 (wt), filled gray bars; DK10409 ( $\Delta pilT$ ), open bars. (b) Velocities obtained from panel a by fitting of a Gaussian (15 and 30 pN) and by fitting of a line to all curves and averaging (60 pN). DK10409, thick-bordered open bars; DK1622 (low-velocity peak), thin-bordered open bars; DK1622 (high-velocity peak), filled gray bars. The error bars indicate standard deviations. (c) Histogram of the stalling forces. DK1622, filled gray bars; DK10409, open bars.

long tail toward higher forces, compared to  $149 \pm 14$  pN in the wt (Fig. 4c). Thus, the PilT-independent retractions in *M. xanthus* are characterized by high velocity and small forces.

## DISCUSSION

**High-force generation is conserved between T4P in *M. xanthus* and *N. gonorrhoeae*.** T4P systems share a core set of 10 proteins, and each system also contains system- and species-specific genes (27). It was therefore unclear whether velocity and force generation in T4P from two very different species would have similar properties. Here, we fully characterized the kinetics and force generation of individual T4P in *M. xanthus* and found that the velocity distributions in both *M. xanthus* and *N. gonorrhoeae* (6) showed a low-velocity mode around  $\sim 700$  nm/s (corresponding to the removal of  $\sim 700$  pilin subunits/s) and a force-dependent high-velocity mode. Skerker and Berg measured the rate of T4P retraction in *P. aeruginosa* at room temperature and found an average velocity in the range of 500 nm/s (30), in good agreement with the average velocity of T4P retraction at room temperature in *N. gonorrhoeae* (B. Maier, A. J. Merz, and M. P. Sheetz, unpublished data). Thus, we conclude that absolute values and bimodal T4P retraction velocity are conserved between different species.

It was unclear whether high-force generation may have evolved with the “lifestyle” of *N. gonorrhoeae* to induce signaling processes in the host cells during infections and to induce cytoprotection and cytoskeletal rearrangements (13). We have shown recently that the maximum force generated by *N. gonorrhoeae* during infections is reduced to  $70 \pm 10$  pN (25), suggesting that the generation of forces that exceed 100 pN has not exclusively evolved to induce signals in the host cells. Furthermore, we previously characterized force generation in an *N. gonorrhoeae* strain in which the major pilin subunit was

replaced by the major pilin subunit of *P. aeruginosa* and found no significant impact on force generation or retraction velocity compared to wt *N. gonorrhoeae* (37). Here, we showed that the force generated by a single pilus of *M. xanthus* even exceeds the force generated by a single pilus in *N. gonorrhoeae*. We therefore conclude that the generation of high molecular force is a conserved physical property of T4P retraction motors independent of the exact components involved in T4P function and of the bacterial lifestyle.

**A PilT-independent mechanism stimulates T4P retraction at high velocity and low force.** Intriguingly, retractions still occurred at a low frequency in a  $\Delta pilT$  mutant in *M. xanthus*. This observation was highly surprising, because the  $\Delta pilT$  mutation has previously been reported to cause a loss of T4P-dependent motility on the basis of an agar plate motility assay (15, 39). Reinspection of our own data (15) in fact provided evidence for a low level of T4P-dependent motility in the  $\Delta pilT$  mutant, i.e., whereas the edges of colonies on an agar surface have a smooth appearance in the  $\Delta pilA$  strain, short flares are observed at the edges of the  $\Delta pilT$  colonies. In light of our new observations, we conclude that this difference in motility is most likely caused by PilT-independent T4P retractions.

The PilT-independent retractions were characterized by high velocities and low forces. The velocity distribution of these retractions matches the distribution in the high-velocity mode observed in the wt. Importantly, we found that the PilT-independent retraction frequency was sevenfold lower than in the wt. Thus, it is unlikely that PilT-independent retractions exclusively account for the high-velocity mode in the wt. We conclude that *M. xanthus* contains a PilT-dependent T4P retraction motor(s) that operates in a low-velocity/high-force mode, as well as in a high-velocity/low-force mode, and a second motor that works only in the high-velocity/low-force mode. At the molecular level, one explanation for the two types of PilT-dependent retractions would be that PilT may bind to separate sites at the base of a pilus.

How does the PilT-independent retraction motor work? Interestingly, analysis of the *M. xanthus* genome identified four genes encoding PilT paralogs (MXAN0415, MXAN1995, MXAN6705, and MXAN6706), which share sequence identities ranging from 37% to 49% and similarities between 43% and 70% with respect to the PilT protein encoded by the *pilT* gene (MXAN5787) in the *pil* cluster. We were unable to identify paralogs for the remaining genes of the *pil* cluster. Precedents for PilT paralogs in other species are the PilU proteins in *P. aeruginosa* and *N. gonorrhoeae*. Inactivation of either *pilT* or *pilU* in *P. aeruginosa* causes a loss of twitching motility (36). In *N. gonorrhoeae*, inactivation of *pilT*, but not *pilU*, causes loss of twitching motility and T4P retractions, and a *pilU* mutant still assembles T4P; however, they do not function normally (26). In principle, the PilT-independent retractions could be spontaneous events. Spontaneous retractions have been proposed for systems including type II secretion systems or the DNA import system of *B. subtilis* that use T4P-like proteins for transport processes across membranes but do not encode PilT homologs (1). Because PilT-independent T4P retractions have not been observed in *N. gonorrhoeae*, we favor the hypothesis that one or several of the PilT paralogs stimulate the PilT-independent retractions. We are currently addressing this

hypothesis by inactivation of the four genes encoding PilT paralogs.

#### ACKNOWLEDGMENTS

We thank Dale Kaiser for providing strains and Kerstin Stingl for helpful discussions.

This work has been supported by the Deutsche Forschungsgemeinschaft, grant MA3898, and the Max Planck Society.

#### REFERENCES

- Allemand, J.-F., and B. Maier. 2009. Bacterial translocation motors investigated by single molecule techniques. *FEMS Microbiol. Rev.* **33**:593–610.
- Balasingham, S. V., R. F. Collins, R. Assalkhou, H. Homberst, S. A. Frye, J. P. Derrick, and T. Tønjum. 2007. Interactions between the lipoprotein PilP and the secretin PilQ in *Neisseria meningitidis*. *J. Bacteriol.* **189**:5716–5727.
- Burrows, L. L. 2005. Weapons of mass retraction. *Mol. Microbiol.* **57**:878–888.
- Chavenet, F., C. Brun, A. L. Banuls, B. Jacq, and R. Christen. 2006. TreeDyn: towards dynamic graphics and annotations for analyses of trees. *BMC Bioinform.* **7**:439.
- Chiang, P., L. M. Sampaleanu, M. Ayers, M. Pahuta, P. L. Howell, and L. L. Burrows. 2008. Functional role of conserved residues in the characteristic secretion NTPase motifs of the *Pseudomonas aeruginosa* type IV pilus motor proteins PilB, PilT and PilU. *Microbiology* **154**:114–126.
- Clausen, M., M. Koomey, and B. Maier. 2009. Dynamics of type IV pili is controlled by switching between multiple states. *Biophys. J.* **96**:1169–1177.
- Craig, L., and J. Li. 2008. Type IV pili: paradoxes in form and function. *Curr. Opin. Struct. Biol.* **18**:267–277.
- Craig, L., N. Volkman, A. S. Arvai, M. E. Pique, M. Yeager, E. H. Egelman, and J. A. Tainer. 2006. Type IV pilus structure by cryo-electron microscopy and crystallography: implications for pilus assembly and functions. *Mol. Cell* **23**:651–662.
- Crowther, L. J., R. P. Anantha, and M. S. Donnenberg. 2004. The inner membrane subassembly of the enteropathogenic *Escherichia coli* bundle-forming pilus machine. *Mol. Microbiol.* **52**:67–79.
- Crowther, L. J., A. Yamagata, L. Craig, J. A. Tainer, and M. S. Donnenberg. 2005. The ATPase activity of BfpD is greatly enhanced by zinc and allosteric interactions with other Bfp proteins. *J. Biol. Chem.* **280**:24839–24848.
- Herdendorf, T. J., D. R. McCaslin, and K. T. Forest. 2002. *Aquifex aeolicus* PilT, homologue of a surface motility protein, is a thermostable oligomeric NTPase. *J. Bacteriol.* **184**:6465–6471.
- Hodgkin, J., and D. Kaiser. 1979. Genetics of gliding motility in *Myxococcus xanthus* (Myxobacterales): Two gene systems control movement. *Mol. Gen. Genet.* **171**:177–191.
- Howie, H. L., M. Glogauer, and M. So. 2005. The *N. gonorrhoeae* type IV pilus stimulates mechanosensitive pathways and cytoprotection through a *pilT*-dependent mechanism. *PLoS Biol.* **3**:e100.
- Hwang, J., D. Bieber, S. W. Ramer, C.-Y. Wu, and G. K. Schoolnik. 2003. Structural and topographical studies of the type IV bundle-forming pilus assembly complex of enteropathogenic *Escherichia coli*. *J. Bacteriol.* **185**:6695–6701.
- Jakovljevic, V., S. Leonardy, M. Hoppert, and L. Søgaard-Andersen. 2008. PilB and PilT are ATPases acting antagonistically in type IV pilus function in *Myxococcus xanthus*. *J. Bacteriol.* **190**:2411–2421.
- Kaiser, D. 1979. Social gliding is correlated with the presence of pili in *Myxococcus xanthus*. *Proc. Natl. Acad. Sci. USA* **76**:5952–5956.
- Kaiser, D., and C. Crosby. 1983. Cell movements and its coordination in swarms of *Myxococcus xanthus*. *Cell Motil.* **3**:227–245.
- Leonardy, S., G. Freymark, S. Hebener, E. Ellehaug, and L. Søgaard-Andersen. 2007. Coupling of protein localization and cell movements by a dynamically localized response regulator in *Myxococcus xanthus*. *EMBO J.* **26**:4433–4444.
- Maier, B. 2005. Using laser tweezers to measure twitching motility in *Neisseria*. *Curr. Opin. Microbiol.* **8**:344–349.
- Maier, B., M. Koomey, and M. P. Sheetz. 2004. A force-dependent switch reverses type IV pilus retraction. *Proc. Natl. Acad. Sci. USA* **101**:10961–10966.
- Maier, B., L. Potter, M. So, C. D. Long, H. S. Seifert, and M. P. Sheetz. 2002. Single pilus motor forces exceed 100 pN. *Proc. Natl. Acad. Sci. USA* **99**:16012–16017.
- Merz, A. J., M. So, and M. P. Sheetz. 2000. Pilus retraction powers bacterial twitching motility. *Nature* **407**:98–102.
- Morand, P. C., E. Bille, S. Morelle, E. Eugène, J.-L. Beretti, M. Wolfgang, T. F. Meyer, M. Koomey, and X. Nassif. 2004. Type IV pilus retraction in pathogenic *Neisseria* is regulated by the PilC proteins. *EMBO J.* **23**:2009–2017.
- Nudleman, E., and D. Kaiser. 2004. Pulling together with type IV pili. *J. Mol. Microbiol. Biotechnol.* **7**:52–62.
- Opitz, D., M. Clausen, and B. Maier. 5 March 2009. Dynamics of gonococcal type IV pili during infection. *Chemphyschem*. doi:10.1002/cphc.200800654.

26. **Park, H.-S. M., M. Wolfgang, and M. Koomey.** 2002. Modification of type IV pilus-associated epithelial cell adherence and multicellular behavior by the PilU protein of *Neisseria gonorrhoeae*. *Infect. Immun.* **70**:3891–3903.
27. **Pellicci, V.** 2008. Type IV pili: e pluribus unum? *Mol. Microbiol.* **68**:827–837.
28. **Ramer, S. W., G. K. Schoolnik, C.-Y. Wu, J. Hwang, S. A. Schmidt, and D. Bieber.** 2002. The type IV pilus assembly complex: biogenic interactions among the bundle-forming pilus proteins of enteropathogenic *Escherichia coli*. *J. Bacteriol.* **184**:3457–3465.
29. **Sakai, D., T. Horiuchi, and T. Komano.** 2001. ATPase activity and multimer formation of PilQ protein are required for thin pilus biogenesis in plasmid R64. *J. Biol. Chem.* **276**:17968–17975.
30. **Skerker, J. M., and H. C. Berg.** 2001. Direct observation of extension and retraction of type IV pili. *Proc. Natl. Acad. Sci. USA* **98**:6901–6904.
31. **Sogaard-Andersen, L., and D. Kaiser.** 1996. C factor, a cell-surface-associated intercellular signaling protein, stimulates the cytoplasmic Frz signal transduction system in *Myxococcus xanthus*. *Proc. Natl. Acad. Sci. USA* **93**:2675–2679.
32. **Spormann, A. M.** 1999. Gliding motility in bacteria: insights from studies of *Myxococcus xanthus*. *Microbial Mol. Biol. Rev.* **63**:621–641.
33. **Sun, H., Z. Yang, and W. Shi.** 1999. Effect of cellular filamentation on adventurous and social gliding motility of *Myxococcus xanthus*. *Proc. Natl. Acad. Sci. USA* **96**:15178–15183.
34. **Sun, H., D. R. Zusman, and W. Shi.** 2000. Type IV pilus of *Myxococcus xanthus* is a motility apparatus controlled by the frz chemosensory system. *Curr. Biol.* **10**:1143–1146.
35. **Thompson, J. D., T. J. Gibson, F. Plewniak, F. Jeanmougin, and D. G. Higgins.** 1997. The CLUSTAL\_X windows interface: flexible strategies for multiple sequence alignment aided by quality analysis tools. *Nucleic Acids Res.* **25**:4876–4882.
36. **Whitchurch, C. B., and J. S. Mattick.** 1994. Characterization of a gene, *pilU*, required for twitching motility but not phage sensitivity in *Pseudomonas aeruginosa*. *Mol. Microbiol.* **13**:1079–1091.
37. **Winther-Larsen, H. C., M. C. Wolfgang, J. P. M. van Putten, N. Roos, F. E. Aas, W. M. Egge-Jacobsen, B. Maier, and M. Koomey.** 2007. *Pseudomonas aeruginosa* type IV pilus expression in *Neisseria gonorrhoeae*: effects of pilin subunit composition on function and organelle dynamics. *J. Bacteriol.* **189**:6676–6685.
38. **Wu, S. S., and D. Kaiser.** 1995. Genetic and functional evidence that type IV pili are required for social gliding motility in *Myxococcus xanthus*. *Mol. Microbiol.* **18**:547–558.
39. **Wu, S. S., J. Wu, and D. Kaiser.** 1997. The *Myxococcus xanthus pilT* locus is required for social gliding motility although pili are still produced. *Mol. Microbiol.* **23**:109–121.